Schweizerische Eidgenossenschaft
Confédération suisse
Confederazione Svizzera
Confederaziun svizra

Federal Department of the Environment, Transport, Energy and Communications DETEC

**Swiss Federal Office of Energy SFOE**
Energy Research and Cleantech

**Yearly Report** December 4, 2023

# ModIceCrys

## CFD Numerical modelling and experimental analysis of ice crystallizers for supercooling flows

INSTITUT FÜR SOLARTECHNIK

OST Ostschweizer Fachhochschule

**Date:** December 4, 2023

**Place**: Rapperswil

**Publisher:**
Swiss Federal Office of Energy SFOE
Research Programme Solar Heat and Heat Storages
CH-3003 Bern
www.bfe.admin.ch
energieforschung@bfe.admin.ch

**Agent:**
Institut for Solar Technology SPF, Eastern Switzerland University of Applied Sciences (OST)
Oberseestr. 10
CH-8640 Rapperswil
www.solarenergy.ch

**Authors:**
Ignacio Gurruchaga, ignacio.gurruchaga@ost.ch
Dr. Daniel Carbonell, dani.carbonell@ost.ch

**SFOE Head of domain:** Andreas Eckmanns, Andreas.Eckmanns@bfe.admin.ch
**SFOE Programme manager:** Stephan A. Mathez, stephan.a.mathez@solarcampus.ch
**SFOE Contract number:** SI/502570-01

# Contents

# List of Acronyms

| | |
|---|---|
| **ASHP** | Air Source Heat Pump |
| **BSI** | Backlight Shadow Imaging |
| **CFD** | Computational Fluid Dynamics |
| **CNT** | Classic Nucleation Theory |
| **DoF** | Depth of Field |
| **GSHP** | Ground Source Heat Pump |
| **PCM** | Phase Change Material |
| **PBE** | Population Based Equations |
| **PBM** | Population Based Model |
| **PIV** | Particle Image Velocimetry |
| **QFV** | Quantitative Flow Visualization |
| **RoI** | Region of Interest |
| **SPF** | Seasonal Performance Factor |
| **TES** | Thermal Energy Storage |
| **TKE** | Turbulent Kinetic Energy |

.

# Glossary

| Notation | Description | Page List |
|---|---|---|
| *attrition* | the process of crystal erosion or breaking into smaller pieces when subjected to stress, e.g. due to collision a high fluid shear | 26 |
| *barrier* | device used to prevent upstream ice propagation. | 15 |
| *BCF theory* | a continuous crystal growth model developed by Burton, Cabrera and Frank in which the dislocations of existing crystals are the source of further growth. | 21 |
| *cavitation* | is the formation (by the reduction of the static pressure of the liquid below the liquid's vapor pressure) and collapse of vapor or gas-filled cavities (bubbles) in a liquid. When the cavities, called "bubbles" or "voids", collapse can generate high-pressure shock waves that can cause nucleation. These shock waves are strong when they are very close to the imploded bubble, but rapidly weaken as they propagate away from the implosion. See *sonocrystallization.* | 15 |
| *Computational Fluid Dynamics* | is a branch of fluid mechanics that employs numerical methods to analyse problems involving fluid flows, chemical reactions or physical processes. | 16 |
| *crystal growth* | second step in crystallization, after *nucleation*, when nucleus once have achieved the critical size, freely and spontaneously increase their size. | 17 |
| *crystallizer* | device that releases the supercooled state of a liquid by promoting nucleation and crystal growth in a controlled manner. | 14 |
| *embryos* | unstable, conglomerates of liquid particles, which may grow depending on local thermal conditions. Stable embryos that have grown larger than the critical radius are called nucleus. | 17, 18 |

| Notation | Description | Page List |
|---|---|---|
| *Gibbs free energy* | the thermodynamic potential that can be used to calculate the maximum amount of work that may be performed by a thermodynamically closed system at constant temperature and pressure, or equivalently, the maximum amount of non-expansion work that can be extracted from a closed system. During crystallization processes the Gibbs free energy change is: $\Delta G = \Delta H - T \cdot \Delta S$ | 18 |
| *ice fraction* | ice fraction is the mass of ice in relation to the total mass of the ice slurry mixture. | 14 |
| *ice slurry* | ice slurry is a pumpable biphasic mixture of small solid ice particles immersed in water or a mixture of water and a freezing point depressant. | 11 |
| *icephobic* | property of preventing the adhesion of ice. | 16 |
| *LM-K theory* | a theory developed by Langer and Müller-Krumbhaar in the 1970s which provided a universal model for dendritic growth rate based on stability criteria. | 21 |
| *metastable* | in thermodynamics, a metastable state is a particularly intermediate phase in a dynamical system towards the lowest, often stable, energy system state. It can also be defined as a state of equilibrium subjected to no more than small disturbances. | 14, 17 |
| *nucleation* | initial formation of embryos, when no ice crystals are present beforehand. This can happen homogeneously within the metastable supercooled liquid itself or heterogeneously originated by a foreign substrate. | 17, 18 |
| *nucleus* | stable embryo. | 17, 18 |
| *phase change material* | a substance capable of undergoing a transition between solid and liquid states at a specific temperature, absorbing or releasing a significant amount of latent heat during this phase transition. PCMs are employed for thermal energy storage, helping to manage and regulate temperatures in various applications, including building construction, electronics, and renewable energy systems. | 11 |
| *polymorphism* | in the context of ice crystals refers to the capacity of ice to be formed in different crystalline forms, depending on factors like temperature, pressure or cooling rate. | 22 |

| Notation | Description | Page List |
|---|---|---|
| *Péclet* | is an adimensional number that is defined as the ratio of the rate of advection (convection) to the rate of diffusion. For example, in fluid flow through a pipe or over a surface, a high Péclet number suggests that the fluid is effectively carrying heat with it, while a low Péclet number suggests that heat is mainly conducted through the material. | 25 |
| *secondary nucleation* | heterogeneous nucleation at the surface of an already existing seed crystal, with different crystal orientation. | 18 |
| *seeding* | introduction of particles into a supercooled fluid to initiate crystal growth. | 15 |
| *solar-ice* | the combination of a solar and heat pump system that uses ice vessels as an intermediate storage device to store solar heat. This system can provide directly from solar to demand or from the solar, throughout the ice storage to the heat pump evaporator when direct solar energy can't fully cover the evaporator's thermal needs. | 8 |
| *sonocrystallization* | triggering nucleation and subsequent crystallization by subjecting supercooled liquid to ultrasonic bombardment. | 15 |
| *Stefan's problem* | formulates the evolution of the movable boundary between the phases of a material undergoing phase change. | 21 |
| *supercooler* | heat exchanger in which the liquid is supercooled. | 14 |
| *supercooling* | cooling a liquid below its melting point temperature without it actually freezing. | 13, 17 |
| *supercooling degree* | temperature difference between the melting temperature and the temperature which the fluid is cooled. | 14, 15 |
| *turbulence enhancer* | device designed to increase or intensify the level of turbulence in a fluid, to improve mixing, heat transfer, and other physical or chemical processes by promoting a more chaotic and vigorous flow within the fluid medium. | 15, 28 |
| *turbulent kinetic energy* | is a physical magnitude used in fluid mechanics that measures the mean kinetic energy associated with eddies in turbulent flow. | 28 |
| *upstream propagation* | propagation of ice against the water flow, typically occurring along walls where the flow velocity is zero. | 15 |

# 1 Motivation

## About the need to bring thermal energy storage to the forefront of research

The bottleneck on the deployment of renewable energy into the heating demands does not lies in the availability of cost-effective generation technologies, where several of them, e.g. solar thermal or heat pumps with photovoltaics are currently cost-effective compared to fossil fuels boilers, but in increasing their contribution to 80 % or 100 % shares of the total demand. To attain this goal, Thermal Energy Storage (TES) need to play a more prominent role, sharing the spotlight with renewable generation technologies.

Solar thermal technology has a huge potential to be used to provide heating demands. For the heating supply on residential applications, the mismatch between the highest solar production (spring, summer or autumn) and the need for space heating supply (winter) leads to the fact that solar thermal needs to be combined it with other technologies, e.g. seasonal thermal storage (not very efficient for small multifamily dwellings), biomass or heat pumps.

Today it is clear that, not only the Swiss energy system, but also the German's, will include a lot of heat pumps to supply residential buildings with heating and cooling. However, which sources these heat pumps will use will depend on many factors such as ground water regulations, social acceptance including the noise of fans for Air Source Heat Pumps (ASHPs) as well as aesthetics, waste water availability, etc. Thus, in order to cover many local and regional needs, several heat sources for heat pumps need to be considered.

In this context, the combination of heat pumps and solar thermal is a very efficient solution, and *solar-ice* system is seen as a substitute for Ground Source Heat Pumps (GSHPs) since it can achieve the same efficiency (Seasonal Performance Factor (SPF)) with the additional benefit of not needing to drill boreholes. When compared to GSHP, solar-ice offers an often missed benefit: it does not need further regeneration in the long term since it regenerates on a yearly basis. Thus, one can see solar-ice systems as equivalent to GSHP systems with full ground regeneration.

An example of the development of the solar-ice technology was implemented within the framework of the European TRI-HP project (`www.tri-hp.eu`), in which several solutions for residential trigeneration (the generation of electricity as well as heating and cooling) were developed and analyzed. As part of this project, a solar-ice slurry storage system, integrated with a natural-refrigerant heat pump was designed to cover electricity, heating and cooling demands in most of the central and northern European climates at least with an 80 % on-site renewable share, thus achieving the objective pursued.

In summary, ice storages integrated into the solar-ice systems exhibit significant potential in residential sector. Additionally, ice storages have a very large variety of other applications, from building cooling using both decentralized or centralized concepts with district cooling networks (Kozawa et al. (2005)) to industrial applications such as breweries and dairies as well as commercial refrigeration for food conservation (Kauffeld et al. (2010)).

## About the need to go one step further on ice storages

The actual technology for ice storages currently named as "ice-on-coil" technology, shown in Figure 1, consists in a vessel using evenly distributed embedded tubes inside.

An anti-freeze heat transfer fluid flows through these tubes causing ice to form on the outer heat transfer surface of the tubes. This approach has the advantage of relative simplicity, without moving parts. However, the embedded tubes represent a significant cost that scales with capacity, making the levelized cost of storage less competitive. In addition, the low thermal conductivity of ice forms a self-insulating layer, which limits the amount of ice that can be formed per unit surface area of tubing. Consequently, other ice storage technologies have emerged, among them, ice slurry technology.

Ice slurry method has the following advantages compared to ice-on-coil method:

- Avoidance of the in-tank heat exchanger where ice is produced with the respective cost reduction.
- Higher melting rates due to the large contact area between ice particles and water.

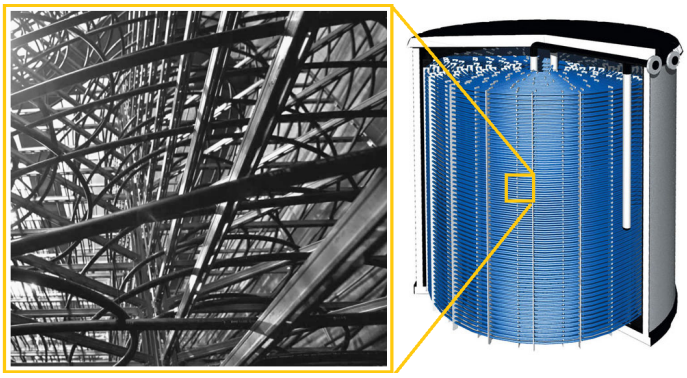

Figure 1: Scheme of different ice-storage tanks using "ice-on-coil" method. Right scheme from Calmac.

- Higher heat pump performance due to the free-of-ice heat exchanger when the ice slurry uses only water. The evaporation temperatures of the refrigerant during ice making will be higher compared to ice-on-coil systems, where the evaporation temperature is decreasing with increasing ice thickness layer.
- No risk of cracking the storage casing due to the expansion of water when freezing and no need to have a structure that keeps the ice immersed, i.e. very cheap vessels, or even rooms or spaces not suitable for residential use in buildings as, e.g. parking spots, can be used to store slurries.
- Avoidance of brine usage as heat transfer fluid in the hydraulic loop between the heat pump and the storage vessel.
- Slurry production and storage take place in two different devices which allows to decouple power requirements and energy storage capability. This provides flexibility for the storage concept, i.e. flexible, cheap and modular storage designs are possible.

## About the state-of-the-art of ice slurry technology production

There are different methods of ice slurry production: fluidized bed, vacuum ice slurry, supercooling and the most commonly used mechanical scraping devices.

The scraper design shown in Figure 2 uses mechanically scraped-surface heat exchangers, where ice is formed on a cold surface and is then removed continuously by a rotating mechanical rod that scrapes ice from a cylindrical barrel. The scraping mechanism creates ice shards that fall to the bottom of the barrel from where are transported away. This ice generating method requires high operation and maintenance cost, and has limited potential for scale up due to the mechanical constrains of the rotating-scraping rod.

For this reason, other ice-slurry production technologies, based on a passive concept for ice slurry production that does not rely on moving parts and that has high efficiency such as the supercooling method combined with a flow-based crystallizer is desirable. The supercooling method involves cooling a substance below its melting point without it undergoing phase transition to the solid phase.

## About the need of modelling and simulation tools for the scalability of crystallizers

The supercooling ice slurry method consists of triggering nucleation, and thus, ice formation, in a supercooled water flow, releasing small ice particles. Ensuring that the supercooling degree (all the sensible energy content) is fully converted into latent energy, i.e. fully exhausted, is a prerequisite to prevent unwanted ice formation in other components of the system. Crystallizers are the key piece of the system where nucleation is triggered and the supercooling degree should be exhausted, with the subsequent crystal growth. The operation of crystallizers, despite the unstable condition of combining supercooling water and ice crystal seeds, can be done in a controlled and reliable way, avoiding upstream ice propagation and exergetic losses.

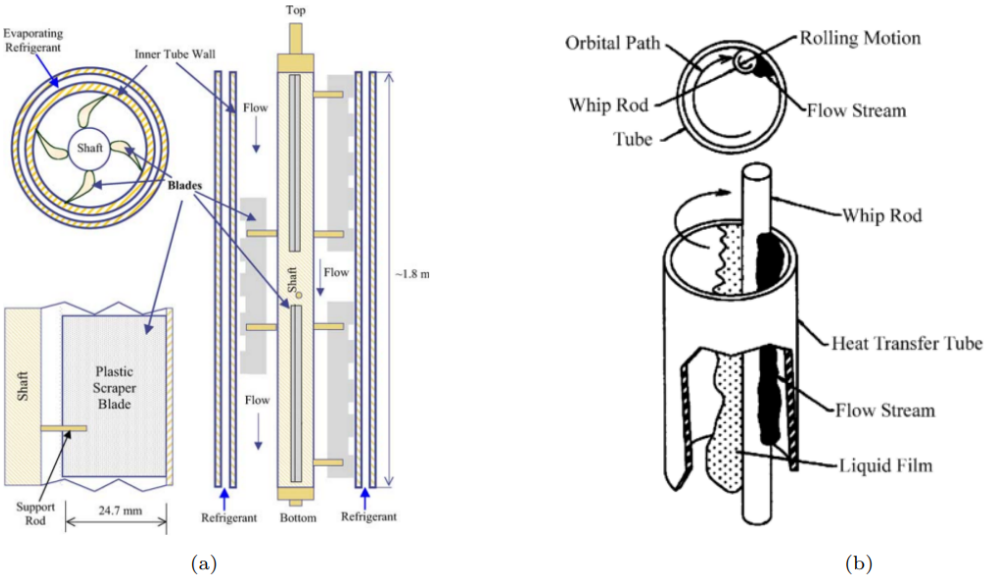


Figure 2: Schematic of ice slurry generators with moving parts, showing a) a scraper type, and b) an orbital rod. Schemes from Stamatiou et al. (2005)

While the background of the physics of ice nucleation is documented on static conditions, little is known on the coupling of supercooled water flows with ice nucleation and growth. Thus, the mathematical modelling of the ice crystallizer is important for a better understanding of the process necessary for a proper scale-up of the technology. Consequently, research on modeling and design tools for the scalability of crystallizers, is required to complete the deployment of the ice slurry technology using supercooling water.

# 2 Objectives

*ModIceCrys* aims to understand the fundamentals of ice growth and its interactions with fluid flows. This know-how will be ultimately used to develop a flow-based ice crystallizer design tool with the aims of Computational Fluid Dynamics (CFD). Thus, a key aspect of the *ModIceCrys* project will be to numerically investigate ice crystallization processes in supercooling water flows. To validate the numerical model experimental assessment of ice crystallizers will be conducted.

The specific objectives of the project are:

1. Develop and validate a numerical model based on Population Based Model (PBM) equations for ice growth in static non-flow conditions.
2. Set-up and validate a Computational Fluid Dynamics (CFD) model of flow-based crystallizer designs without the ice crystallization process.
3. Develop a numerical framework based on CFD able to predict the fluid flow behaviour, ice crystallization process and ice crystal growth and the coupling between fluid flow and crystallization.
4. Experimentally evaluate two crystallizer designs to validate the CFD model.

# 3 Work carried out

## 3.1 Introduction

During 2023, the main work carried out for the project *ModIceCrys* was, on one hand, finishing the contextualization of the object of research in the whole framework of thermal storage technologies and solar ice slurry production systems, on the other hand, finishing the literature review on ice slurry, crystallization theory and models, crystallizers, and CFD Multiscale and coupling with PBM.

In the following sections, a summary of the investigations for each topic is provided.

## 3.2 Contextualization

A general overview of the contextualization can be visualized in the following diagram.

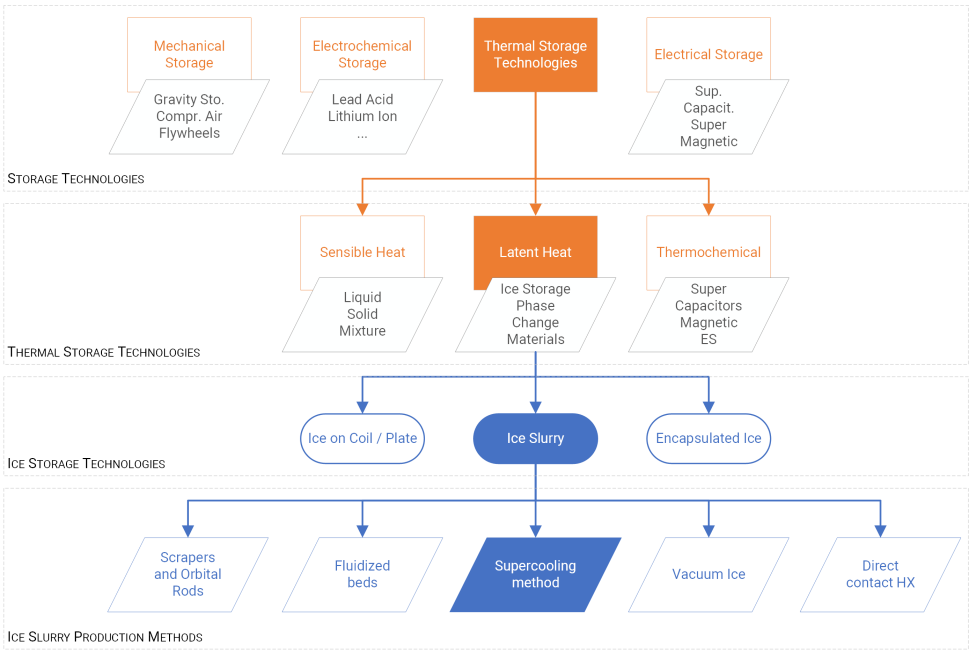


Figure 3: Thermal Storage Technologies. Ice Storage Technologies and Ice Slurry production methods.

## 3.3 Ice slurry technology

*Ice slurry* is a biphasic mixture of small solid ice particles immersed in the water fluid, thus, at an equilibrium temperature of 0 °C. Ice slurry is *phase change material* (PCM) with a very high latent energy considering its low melting temperature, and thus, it can be used as a high energy density storage medium. Additionally, ice slurry is a pumpable biphasic mixture, so it can be used not only as a storage medium but also as a heat transfer fluid.

The maximum ice mass fraction's content in ice slurry, which is limited due to the geometrical shape of ice crystals and the surrounding water, is around 60 %. In practice, commercial ice slurry Japanese systems reported in the literature using water supercooling do not achieve mass fractions beyond 50 %. This value is lower compared to the 80 % value that ice-on-coil storage technology could achieve safely. However, in practice, typical ice-on-coil systems installed in Switzerland rarely go beyond 60 % approximately.

Considering an ice mass fraction of 50 %, a storage energy density of 167 kJ/kg can be achieved, compared to 4.18 kJ/(kg K) of water sensible heat storage achieved per each Kelvin of temperature difference. Considering a case where $\Delta T = 10$ K, the thermal energy density per unit mass of the ice slurry would be around 4 times higher than that of the hot water sensible storage tank.

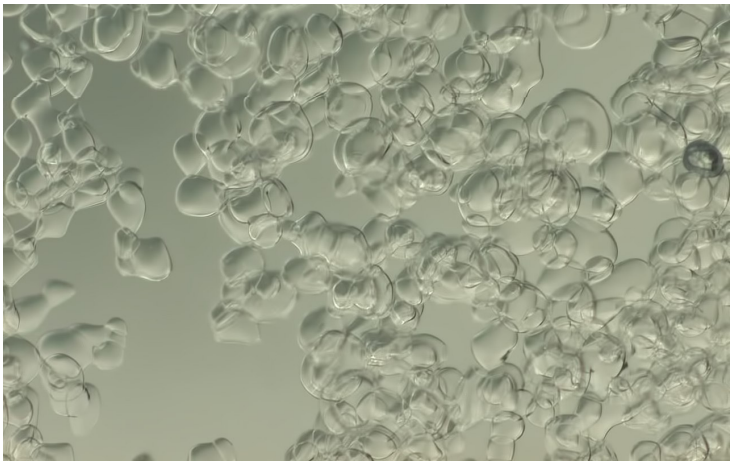

Figure 4: Ice slurry under microscope.

### Ice slurry production methods

The production of ice slurry can be achieved in multiple ways (Kauffeld et al., 2005a, Mouneer et al., 2010, Zhang and Ma, 2012):

- **Scraper design** includes a moving scraper that periodically or continuously remove the ice crystals from a heat exchanger wall. It is one of the simplest and most common methods, but involves moving parts, and requires motor power. Its scalability is limited due to the force acting on the scraper arm and the required motor power.
- **Orbital rod generators** work similar to the scraper design. A moving whip rod is used to de-ice the surface, which is commonly the inner wall of a tubular heat exchanger. Unlike the scraper design, it does not touch the exchanger walls and usually moves much faster compared to the scrapers.
- **Fluidized bed generators** use movings beads whirled inside the fluid flow. These beads randomly hit the heat exchanger wall removing the ice crystals that grow on the wall surface.
- **Supercooling method** separates the location of cooling and nucleation. Thus, ice does not grow on the heat exchanger surface and no moving parts are needed. However, prevention of spontaneous nucleation within the system is a challenge.
- **Direct contact heat exchangers** benefits from a large heat transfer between the icing fluid and the immiscible refrigerant which are in direct contact. As the icing fluid transfers heat to the refrigerant, the latter evaporates and can be then removed from the freezing fluid.
- **Vacuum ice slurry generation** works using states close to the triple point of water. Cooled water is sprayed into a deep vacuum, such that part of the water evaporates. The latent heat of vaporization is removed from the remaining liquid water, which then freezes.

From the methods above, the most efficients are the vacuum ice and the supercooling methods. The supercooling method does not require additional energy and does not utilize moving parts.

## 3.4 Supercooling ice slurry system

### Supercooling method

The *supercooling* method, as shown in Fig. 5, involves cooling a substance below its melting point without it undergoing phase transition to the solid phase. Significant supercooling is normally achieved by using small samples e.g, droplets in static conditions where the cooling rate is controlled. On real applications one might try to avoid high turbulent flows and to remove nucleation sites, such as impurities or bubbles, that could initiate crystallization.

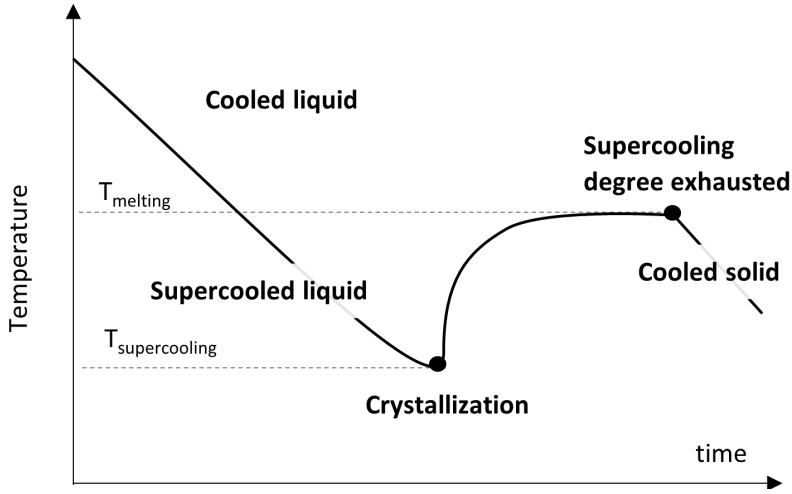


Figure 5: Evolution of temperature as a function of time in the supercooling method.

### Supercooling flow-based crystallizer system

A scheme of the supercooling flow-based crystallizer system to produce ice slurries is shown in Figure 6.

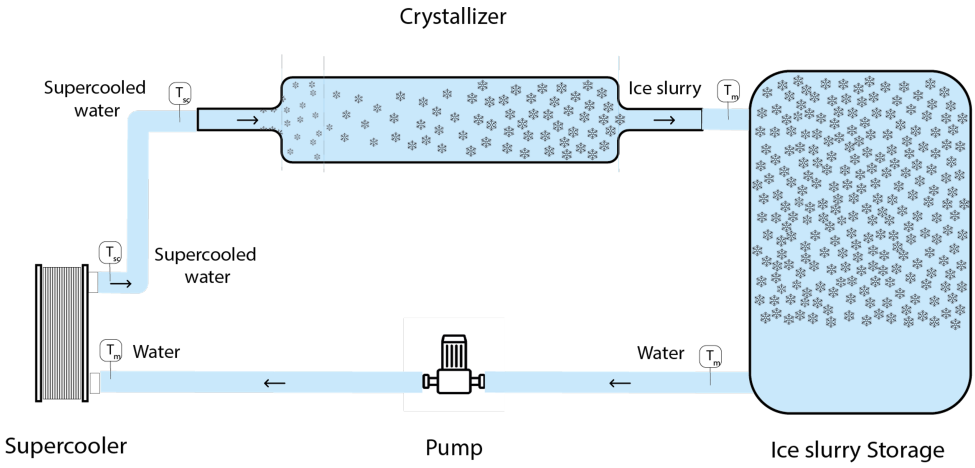


Figure 6: Simplified concept scheme of the ice slurry supercooling concept: water is supercooled by a chiller and the ice slurries are generated into the crystallizer to be stored in the ice storage.

The basic concept can be described in the following manner: starting from the *pump*, liquid water at the melting temperature (0 °C) is pumped to the *supercooler* where it undergoes supercooling obtaining *supercooled water*. Right after the supercooling, the flow is induced to nucleate in a controlled manner in what is called a *crystallizer*. In the crystallizer, not only the nucleation is triggered but also all supercooling sensible heat must be converted into latent energy, and thus solid crystals are formed using this sensible heat energy, becoming the mixture of water and ice particles at 0 °C. Since the ice slurry should not supercooled anymore after the crystallizer, it cannot freeze anywhere else, thus avoiding clogging and unwanted nucleation in other parts of the system.

In the crystallizer, the converted liquid into solid mass fraction depends on the *supercooling degree* $\Delta T_{sc}$, the enthalpy of fusion $h_{fus}$ and the heat capacity of the fluid phase $c_{p,l}$.

$$m_{l,i} \cdot c_{p,l} \cdot \Delta T_{sc} = m_{s,o} \cdot h_{fus} \tag{1}$$

For ice slurry with a supercooling degree of 2 K, the amount liquid mass that is converted into solid, the mass *ice fraction*, is ca. 2.5 %. Therefore, this cycle can be repeated continuously until reaching the maximum mass ice fraction in the ice slurry storage, typically, around 50 %.

#### Development status of supercooling ice slurry production method

The development of the ice slurry technology using the supercooling method has three main challenges:

1. Supercooling water below 0 °C in stable form in the *supercooler*.
2. Crystallizing water in a controlled manner avoiding upstream ice propagation and release all the supercooling potential in the *crystallizer*.
3. Pumping and storing slurries without clogging with proper separation from liquid water and solid particles in the storage vessel.

The first challenge has been mostly covered within the H2020 project TRI-HP where icephobic coatings have been developed and demonstrated to increase supercooling degree by up to 40 % compared to untreated heat exchangers (Carbonell et al., 2022). These supercoolers have been used in TRI-HP with real heat pumps of 10 kW using propane and $CO_2$ as refrigerants successfully. One of these supercoolers has been used extensively in the test rig of the SFOE SlurryStore project (Carbonell et al., 2023). The second challenge was approached in the aforementioned SlurryStore project, where several crystallizer designs were tested. Although a lot of practical experience was gained, the design of a functional crystallizer led to very high thermal losses and low crystallization power. For the design of the crystallizer, a try-and-error methodology was followed, which turned out to be not the best approach. The present work aims to tackle this problem with a science-based approach. The third challenge of ice slurry management, including proper vessel design to store the slurries, was the aim of the SlurryStorage project. We achieved some functional designs, however, there will be a need for further research work for a proper scale-up.

## 3.5 Crystallizer

The *crystallizer* plays a crucial role in the supercooling flow-based ice slurry system, where the supercooled water is converted into ice slurry. In the crystallizer, not only the nucleation is triggered, but also all supercooling sensible heat must be converted into latent energy, and thus solid crystals are formed using this sensible heat energy, resulting in a mixture of water and ice particles at 0 °C as it exits the crystallizer.

Supercooling is a *metastable* state, which can be altered by any disturbance of the boundary conditions. It is precisely in the crystalliser, and in no other part of the system, where we want to promote and realize this change of state, from metastable to stable, i.e. from supercooling liquid to ice slurry. The main challenge is to control *where* and *how* the ice is formed. That leads to three challenging guidelines for the crystallizer design:

- **Induce crystallization**. Provoke ice formation in crystallizer by promoting ice nucleation (Beaupere et al., 2018), using the supercooling degree as the main driver.

- **Maximize crystallization potential**. Exhaust the *supercooling degree* in the crystallizer and reduce the required resident time by enhancing turbulence.

- **Prevent upstream ice propagation**. Avoid or reduce the formation of ice on the surface of the crystallizer which could travel upstream clogging the supercooler heat exchanger.

### 3.5.1 Actual crystallizer design

A scheme of a current crystallizer concept is shown in Figure 7.

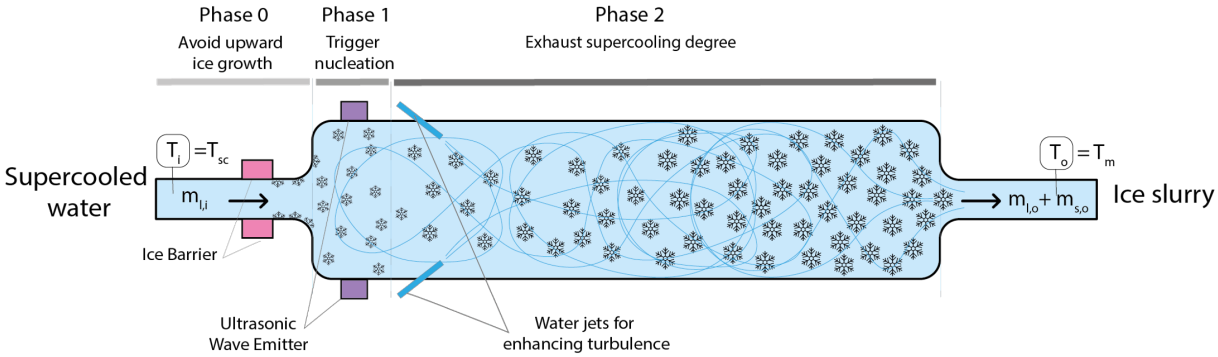


Figure 7: Scheme of current ice crystallizers.

The concept is as follows: the first ice particles are generated due to the *cavitation* induced by the ultrasound device placed at the inlet supercooled water flow rate, *Phase 1 Trigger nucleation*. The process of generating ultrasound waves is known as ultrasonic bombardment. Cavitation produces small bubbles, and their implosion generates a shock wave that initiates nucleation, known as *sonocrystallization*. Nevertheless, some particles are formed just over the walls, where the flow velocity is zero. Despite the flow pushing the growing ice from the walls away, some micro-particles are kept on the walls, having opposite consequences. On one hand, makes the ice slurry production possible even if the ultrasonic transducer is not operating, as these ice particles on the walls act as *seeding* for the continuous crystallization process. On the other hand, independent of the bulk flow rate velocity, as the wall flow velocity is zero, crystals tend to grow towards the highest supercooling gradient, thus towards the supercooler upstream, endangering the integrity of the system in case of clogging. To avoid *upstream propagation*, the system integrates a *Phase 0* based on a double water jacket as a ice *barrier*, which maintains the wall over 0 °C, avoiding freezing to grow through the wall.

The shape of ice formed in *Phase 1 Trigger nucleation* is pushed away to *Phase 2 Exhaust supercooling degree* in this design like a ring since ice grows on the walls. As this shape makes the pumping very difficult and needs to be broken, a water jet at 0 °C is introduced, which enhances turbulence apart from breaking the ice ring at a cost of increasing exergetic losses and reducing the overall crystallization efficiency.

The first crystallizer design developed under the SlurryStore Project operates at $T_{sc}$=2 °C and with a mass flowrate of 400 kg/h, consequently at a nominal power of 0.9 kW. Double water jacket ice *barrier* exergetic losses were estimated in 0.1 kW. Water jets, acting as a ice ring breaker and *turbulence enhancer*, resulted in exergetic losses of 0.3 kW. The crystallizer net power, discounting all losses is about 0.44 kW, the 50 % of the nominal power.

The last crystallizer design developed under the SlurryStore Project operates at $T_{sc}$=1 75 °C and with a mass flowrate of 1250 kg/h, consequently at a nominal power of 2.54 kW. Ice barrier exergetic losses were estimated in 0.2 kW. The last crystallizer design improved the water jets *turbulence enhancer* into a concentric pipe mixer, resulting in exergetic losses of 0.3 kW. The crystallizer net power, discounting all losses is about 1.8 kW, the 70 % of the nominal power for this last design.

### Concept idea of crystallizer enhanced design

The current designs of crystallizers face significant limitations in terms of efficiency, and more notably, they pose difficulties when attempting to scale up to higher capacities in a cost-effective manner.

For this reason, under the same design criteria outlined in **??**, proposed solutions or enhancements to the design and operating conditions are proposed. These solutions are resumed in the following table:

| Criteria | Solution |
|---|---|
| Exhausting supercooling degree while reducing residence by means of increasing number of nucleus | Increase $\Delta T_{sc}$ (up to 4 K)<br>Increase the number of nucleus. Ultrasound devices<br>Increase the number of nucleus. Physical trigger<br>Increase the number of nucleus. Recirculation |
| Exhausting supercooling degree while reducing residence by means of enhancing turbulence | Increase the number of nucleus. Bubbling<br>Introduce fixed physical baffles with *icephobic* coatings<br>Introduce movable physical baffles with *icephobic* coatings<br>Stirred crystallizer<br>Improve performance of the actual water jet system |
| Avoiding upstream ice propagation | Introduce *icephobic* coatings<br>Increase ultrasound devices all over the wall<br>Create a discontinuity air layer<br>Introduce a flexible or movable inlet<br>Improve performance of the actual ice barrier |

Table 2: Overview of concept ideas for upscaling the crystallizer.

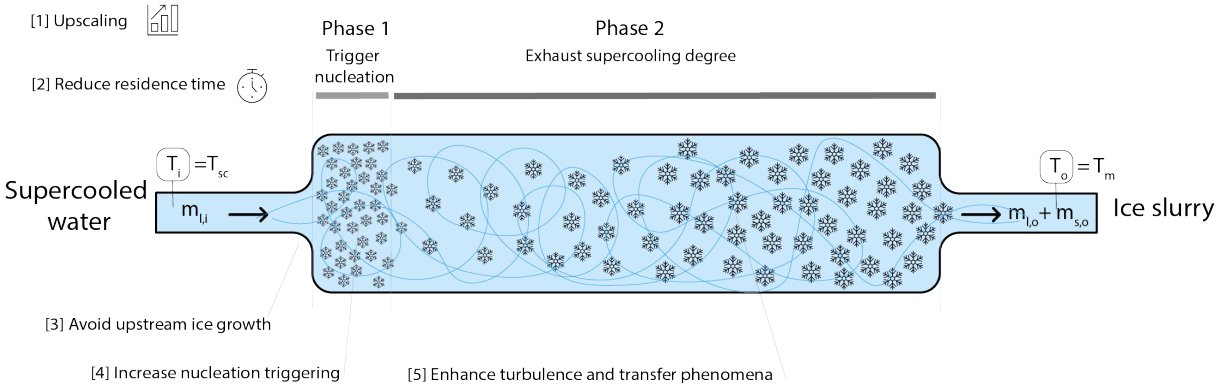


Figure 8: Concept idea for new ice crystallizer design.

The present work will centre around studying these different solutions with the goal of designing a crystallizer which aims to operate in a controlled manner, preventing upstream ice propagation, and achieving high-efficiency supercooling release. To do so, it is necessary to understand the fundamentals of ice nucleation and crystal growth and its interactions with fluid flow dynamics in order to develop a flow-based ice crystallizer design tool with the aims of CFD (*Computational Fluid Dynamics*).

## 3.6 Crystallization

### 3.6.1 Introduction

Freezing or solidification is the physical process where liquids turn into a solid when decreasing their internal energy, normally by cooling, lowering their temperature below the freezing point. Melting is the inverse physical process where a solid substance turns into a liquid when increasing its internal energy, typically by raising its temperature above the melting point. The melting point is the temperature where the solid and liquid phases of a substance coexist in equilibrium.

For all substances, there is some hysteresis between the freezing and melting temperatures that are observed, which we refer here as supercooling. For most, this is small and the two are in near agreement, and for others, the difference is larger. The origin of this difference is merely that the formation of the solid phase is kinetically hindered by an increased activation energy barrier as well as by mass transfer limitations for crystal growth.

Most liquids freeze (or solidify) by *crystallization*, which is the process in which the disorganised atoms or molecules of a substance in a liquid state transform into a highly organised solid structure, known as a crystal. Water, which is one of the most abundant substances on Earth and has an essential role in life, crystallizes into ice, that's to say, freezes or solidifies forming a well-organised solid structure. Only under special nanoconfinement, by means of an experimental setup, water may be prevented from crystallizing into a hexagonal structure (Salvati Manni et al., 2019) and forming amorphous water over ice. Otherwise, there are substances that normally solidify without crystallization, forming amorphous solids (i.e. glass).

Despite crystallization may occur by freezing, as in the case of water, by lowering its temperature under the freezing point, crystallization may also occur through other physical or chemical processes, such as precipitation from a supersaturated solution or deposition from a gas.

The decrease in temperature below the freezing point of those crystallizing substances is not the only condition to be met for triggering crystallization. The freezing into a crystal may occur at a temperature slightly, or even significantly below, its freezing temperature. When a substance is cooled below its melting point and is still liquid it is said the substance is in *supercooling* state.

The *supercooling* condition of water is a *metastable* state, which means it is an intermediate state that can be disturbed easily in order to evolve towards a stable state in which ice is formed.

The phase change inherently involves the creation of an interface between the two phases, liquid and solid, which in turn requires of an activation energy, an additional energy step. That is the reason for the existence of liquid water below its freezing point, named as *supercooled water*. Supercooled water exists in nature: droplets of supercooled water exist in cumulus clouds and some animals or plants depend on this physical phenomenon to survive to extreme temperatures.

Crystallization consists of two processes: *nucleation* and *crystal growth*. Nucleation is the first step where ice *embryos* are formed in the supercooled liquid. The second step, in which the size of the crystal *nucleus* increases, is known as *crystal growth*.

Crystallization depends on intermolecular, intramolecular forces and its kinetics and thermal diffusion processes (Libbrecht, 2017).

### 3.6.2 Nucleation

There are two different nucleation mechanisms: *homogeneous* and *heterogeneous* nucleation.

- The *homogeneous nucleation* occurs spontaneously in the aforementioned metastable state of supercooled water when stochastic spatial fluctuations form "isolated singularities" of water molecules, called *embryos* which transform into ice (Dorsey, 1948). These embryos, depending on size and shape, may decay and redissolve into the parent phase again, or grow, and turn into a stable *nucleus*, depending on the local balance of the *Gibbs free energy* of nucleation (Kauffeld et al. (2005b)).
- The *heterogeneous nucleation* initiates from a foreign substrate (a boundary such as a wall, another particle or seed in the aqueous solution). A special case of heterogeneous nucleation is the *secondary nucleation* where nucleation is triggered by a previously formed crystal.

*Homogeneous Nucleation*

The Classic Nucleation Theory (CNT) explains *nucleation* in terms of Gibbs free energy, considering two counteracting free energy factors: the volume free energy, $\Delta G_V$, J, and the surface free energy $\Delta G_S$, J, (Fisher et al., 1949). During the phase transition from water to ice state, the Gibbs free energy of the *liquid* water molecules is released due to the lower free energy of *solid* ice, while some free energy is required for the creation of a new interface that splits the two phases: water and ice. The expression reads as:

$$\Delta G = -\Delta G_V + \Delta G_S \tag{2}$$

In the case of the formation of a small ice nucleus with a spherical shape from a purely metastable state in homogeneous nucleation, the expression can be rewritten as the following:

$$\Delta G = -V\ \Delta G_{V'} + A\ \Delta G_{S'} = -\frac{4}{3}\pi r^3\ \Delta G_{V'} + 4\pi r^2\ \gamma_{iw} \tag{3}$$

where $\Delta G_{V'}$ and $\Delta G_{S'}$ are volume and surface free energy in relative volume and area units respectively $\Delta G_{V'}$ is in J/m$^3$, $\Delta G_{S'}$ in J/m$^2$, $r$ is the radius of the small nucleus, m and $\gamma_{iw}$ is the interfacial tension, J/m$^2$, (the surface free energy required) between the small nucleus and the supercooled water.

For the volume of free energy released by the small nucleus, the general expression for the change in Gibbs free energy can be used, where $\Delta H$ is enthalpy, J, $T$ the temperature, in K and $\Delta S$ is entropy J/K:

$$\Delta G_{V'} = \rho \cdot (\Delta H - T \cdot \Delta S) \tag{4}$$

Developing the previous:

$$\Delta G_{V'} = \rho \cdot ((H_{wat} - H_{ice}) - T_{sc} \cdot (S_{wat} - S_{ice})) = \rho \cdot (\Delta h_{fus} - T_{sc}\frac{h_{fus}}{T_m}) = \rho \cdot h_{fus}(1 - \frac{T_{sc}}{T_m}) = \frac{\rho\ h_{fus}\Delta T_{sc}}{T_m} \tag{5}$$

where $wat$ and $ice$ subindexes refer to water and ice respectively, $\rho$ is the density of water, kg/m$^3$, $h_{fus}$ is the enthalpy of fusion, J/kg, $T_m$ the melting temperature, K, $T_{sc}$ the supercooled water temperature, K, and $\Delta T_{sc}$ the supercooling degree $T_m - T_{sc}$. Substituting in equation (2):

$$\Delta G = -\frac{4}{3}\pi r^3\ \frac{\rho\ h_{fus}\Delta T_{sc}}{T_m} + 4\pi r^2\ \gamma_{iw} \tag{6}$$

From the previous expression, it can be stated that homogeneous nucleation depends basically on the supercooling degree $\Delta T_{sc}$ and interfacial energy between ice and water $\gamma_{iw}$. In Fig. 9, it is shown how different free energy for nucleation are required depending on different interfacial energy between ice and water $\gamma_{iw}$.

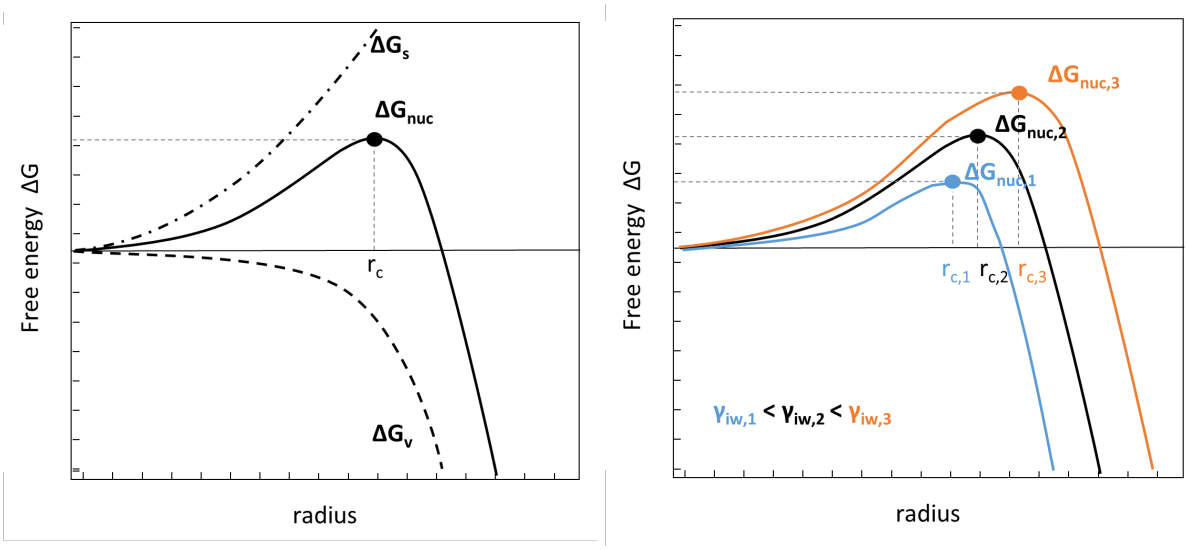


Figure 9: *Left*: Sketch of the free energy of nucleation composed by the balance of volume and surface Gibbs free energy. The critical radius $r_c$ for homogeneous nucleation is derived for $\partial(\Delta G)/\partial r = 0$. Spontaneous crystal growth starts from $\Delta G < 0$, previously the free energy of nucleation $\Delta G_{nuc}$ should be met for achieving the $r_c$. *Right*: Different free energy of nucleation $\Delta G_{nuc,1,2or3}$ result depending on different interfacial energy between ice and water $\gamma_{iw,1,2or3}$

For obtaining the critical radius $r_c$, above which the nucleation process releases energy and the spontaneous growth of the nucleus occurs, the Eq. 6 is derived for $\partial(\Delta G)/\partial r = 0$ obtaining.

$$r_c = \frac{2\ \gamma_{iw}\ T_m}{\rho\ h_{fus} \Delta T_{sc}} \tag{7}$$

The free energy of nucleation $\Delta G_{nuc}$ is the amount of free energy required for creating the minim nucleus with the potential to grow, which equals the energy required for creating the interface minus the energy released. Thus, $\Delta G_{nuc}$ is obtained replacing the $r_c$ from Eq. 7 into the $r$ in 6 resulting in:

$$\Delta G_{nuc} = \frac{16\pi}{3} \frac{\gamma_{iw}^3\ T_m^2}{(\rho\ h_{fus} \Delta T)^2} \tag{8}$$

Assuming an ice water interfacial energy $\gamma_{iw}$ of 29.1 J/m$^2$ (Němec (2013)) the critical radius and the values of the nucleation energy are shown in Table. 3.

Table 3: Critical radius and free energy of nucleation for homogeneous nucleation.

| **Temperature** $T$ °C | **Critical radius** $r_c$ nm | **Number of molecules** $n$ - | **Energy of nucleation** $\Delta G_{nuc}$ J |
|---|---|---|---|
| -40 | 1.19 | 71 | 5.20657E-14 |
| -20 | 2.38 | 733 | 2.68303E-13 |
| -5 | 9.54 | 46710 | 4.27165E-12 |
| -3 | 15.9 | 217083 | 1.19113E-11 |
| -2.5 | 19.08 | 375119 | 1.71523E-11 |
| -2 | 23.85 | 732654 | 2.68006E-11 |
| -1.5 | 31.79 | 1736662 | 4.76455E-11 |
| -1 | 47.69 | 5861234 | 1.07202E-10 |

Derivations of Eq. 6, Eq. 7 and Eq. 8 must be considered only for the assumption of the spherical shape of small embryos or nucleus. For other non-spherical-like aspect assumptions as in the case of nucleation of

needle, disks or platelet-like crystals, other equations could be derived as presented in Giberti (2014). As a consequence, different solutions of $r_c$ and $\Delta G_{nuc}$ would be obtained as shown in Fig. 10.

Indeed, in the same reference (Giberti (2014)) another way of expressing the equation (6) in terms of the number of constituents (number of molecules) instead of the critical radius $r_c$ is chosen, and converts that expression into a geometrical-shape-independent formulation, which is more useful in case of polymorphism.

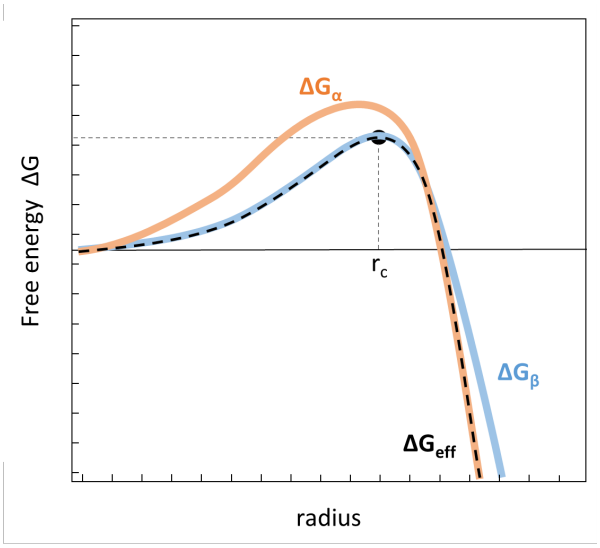


Figure 10: Two polymorphism, $\alpha$ and $\beta$ possess two different free energy of nucleation $\Delta G_{nuc}$. $\alpha$ is more stable than $\beta$, and consequently, when nucleation occurs, the first polymorph to nucleate is $\beta$, which turns into $\alpha$ as soon as the two resulting free energy curves cross each other ($\Delta G_{eff}$).

*Heterogeneous Nucleation*

For heterogeneous nucleation, which describes nucleation at foreign surfaces, the free energy of nucleation is lower than that of homogeneous nucleation by a factor $0 \leq f \leq 1$ that depends on the interface and the geometry of the surface.

$$\Delta G_{het} = f \cdot \Delta G_{nuc} \tag{9}$$

For the simplified case of a smooth surface shown in Fig. 11 the $f$ can be expressed in terms of the wetting angle $\theta_{wett}$:

$$f = \frac{1}{4}(2 + cos\ \theta_{wett}) \cdot (1 - cos\ \theta_{wett})^2 \tag{10}$$

The $cos\ \theta_{wett}$ depends on interfacial energy between ice and water $\gamma_{iw}$, and likewise for every water's phase with the surface $\gamma_{isurf}$ , $\gamma_{wsurf}$, in agreement with Young's equation:

$$cos\ \theta_{wett} = \frac{\gamma_{wsurf} - \gamma_{isurf}}{\gamma_{wi}} \tag{11}$$

For wetting angles of $\theta_{wett} = \frac{\pi}{2}$, $f = 0.5$ and then $\Delta G_{het} = 0.5 \cdot \Delta G_{nuc}$, thus, resulting in heterogeneous nucleation being half of the homogeneous equivalent. This lowered energy step involves that heterogeneous nucleation requires normally lower degrees of supercooling (or supersaturation) compared to homogeneous nucleation.

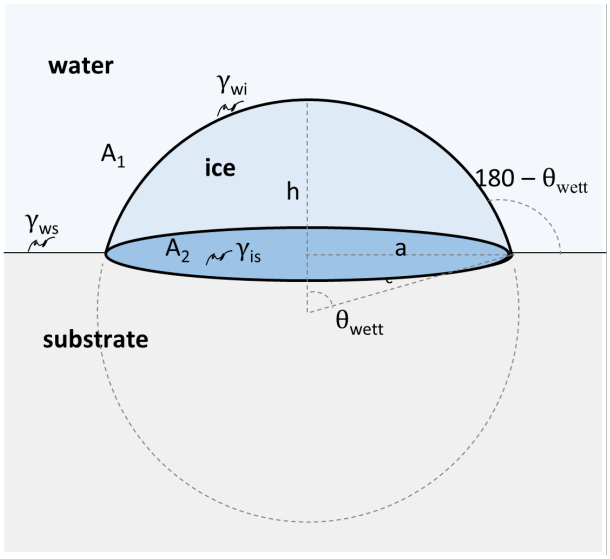


Figure 11: Surface balances for heterogeneous nucleation.

### 3.6.3 Crystal growth

The crystal growth mechanisms have been a question of interest for decades. Since J.W. Gibbs settled the basis of the thermodynamic equilibrium applied to chemical reactions and phase transitions by the end of 19$^{th}$ century (Gibbs, 1879), crystal growth has been the main topic of a vast number of researchers.

Since mid 20$^{th}$ century, there was an increasing number of investigations, both experimental and theoretical, which were conducted to explore the thermophysical and kinetic dependencies of crystal growth rates. Burton, Cabrera, and Frank developed the *BCF theory* in the 1950s (Burton et al., 1951), which provided a fundamental framework for understanding crystal growth by atomic processes approach. Other researchers like Dorsey (1948), Fisher et al. (1949) or Cahn et al. (1964) assumed a power-law-type relationship between the velocity growth rate $v$ and bulk supercooling temperature $T_{sc}$ in the form: $v = a \cdot \Delta T_{sc}^{b}$, where $a$ and $b$ were empirically determined, resulting in empirical correlations that effectively captured the experimental data. These first experiences were useful in providing the first experimental crystal growth references, but their universal applicability beyond the framework of their experimental conditions (fluid material, fluid velocities, supercooling temperatures, experimental setups, etc.), was a matter of questioning and continuous further research. Furthermore, these empirical expressions, although useful, offered limiting profound insights into the intrinsic crystal growth process.

Papapetrou is credited with solving, in 1935, the growth rate for a dendrite with a cylindrical tip Akhtar et al. (2021), Kurz (2017), Wang et al. (2019). However, this contradicted experimental observations that favoured a parabolic tip shape. Ivantsov (1947) addressed this by formulating the *Stefan's problem* and solving the dendritic growth for a parabolic tip shape in 1947. Nevertheless, his solution was valid only for a range of values for the dendritic growth rate and dendritic curvature radius.

In the 1960s-1970s, experimental studies on crystal growth gained relevance: advances in experimental techniques, including microscopy and controlled environment experiments, allowed scientists to observe and measure crystal growth more accurately e.g. (Fernandez and Barduhn, 1967). Kallungal and Barduhn (1977) considered the flow velocity $V$ in the form: $v_{tip} = a \cdot \Delta T_{sc}^{b} \cdot V^{c}$ on the traditional power-law-type relationship between growth rate of the tip dendrite $v_{tip}$ and bulk supercooling temperature. Likewise, the coefficients $a$, $b$ and $c$ were empirically determined by fitting the experimental data.

The *LM-K theory*, which takes its name from its authors: Langer and Müller-Krumbhaar, provided a universal model for dendritic growth rate based on stability constant in the 1970s, Langer and Müller-Krumbhaar (1977), Langer et al. (1978) and Langer and Müller-Krumbhaar (1978). This theory contributed to the un-

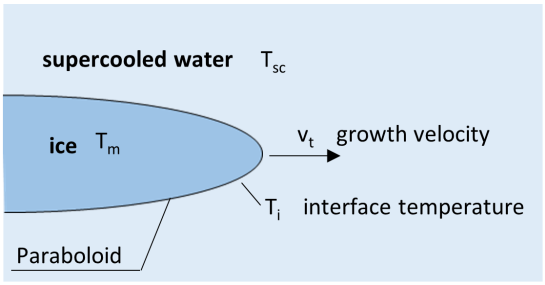


Figure 12: Dentrite crystal form as a paraboloid of revolution.

derstanding of dendritic growth in various materials. This model was an important landmark but did not include curvature effects or molecular kinetics, which appear to be significant limitations to the model beyond a supercooling temperature.

To solve this limitation to the LM-K theory, Shibkov highlighted the need to consider the transition from diffusion to kinetics limited regimes at higher supercooling degrees, prompting the need to incorporate kinetic effects. This *crossover*, using Shibkov's own term, from diffusion to kinetics limited growth rate of ice crystals occurs above a supercooling temperature $\Delta T_{sc} > 4$ K to 5 K (Shibkov et al., 2005, 2004). A couple of years before, Shibkov had also analysed the *polymorphism*, the dependence between the different macroscopic structures: dendrite, needle-like crystal, fractal needled branch or platelet, and the supercooling degree in a morphology diagram of growth patterns (Shibkov et al., 2003). These different morphologies and growth patterns of ice are shown in Fig. 13 as a function of the supercooling degree $\Delta T$.

In Fig. 14 it can be seen that below a certain supercooling temperature, the LM-K theory is valid and reproduces the experimental data correctly. Based on that, it can be stated that for low supercooling rates, the diffusive heat transfer effect is the limiting factor for crystal growth, while for higher supercooling temperatures, the limiting factor is related to molecular kinetic. Thus, for higher supercooling degrees, regardless the morphology, what should be considered is the kinetic effect of the crystal's growth rate.

These kinetic effects in dendritic growth can be addressed by means of the linear kinetic theory or by means of the Wilson-Frenkel model. As described by Akhtar et al. (2021): *"While both theories consider the effect of attachment kinetics in their formulation, the Wilson-Frenkel model has been demonstrated to predict the growth rates well for liquids with Lennard-Jones potential such as water."* Other authors, Wang et al. (2019) have suggested similar solutions, by modifying the interface temperature, in order to add the kinetic limitation.

Although the LM-K theory is flawed for its non-consideration of the kinetic effects, which would not be suited for higher supercooling degrees, for applications where the $\Delta T$ is below 4 K, it is accurate enough.

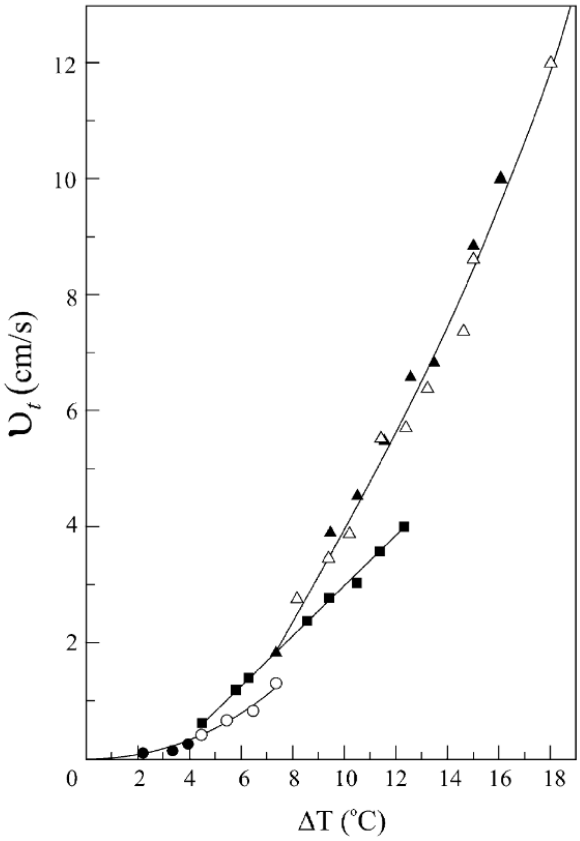


Figure 13: Morphology diagram of growth patterns from Shibkov et al. (2003). (•) Dendrite, (○) needle-like crystal, (■) fractal needled, (△) compact needled or (▲) platelet, depending on supercooling degree $\Delta T$.

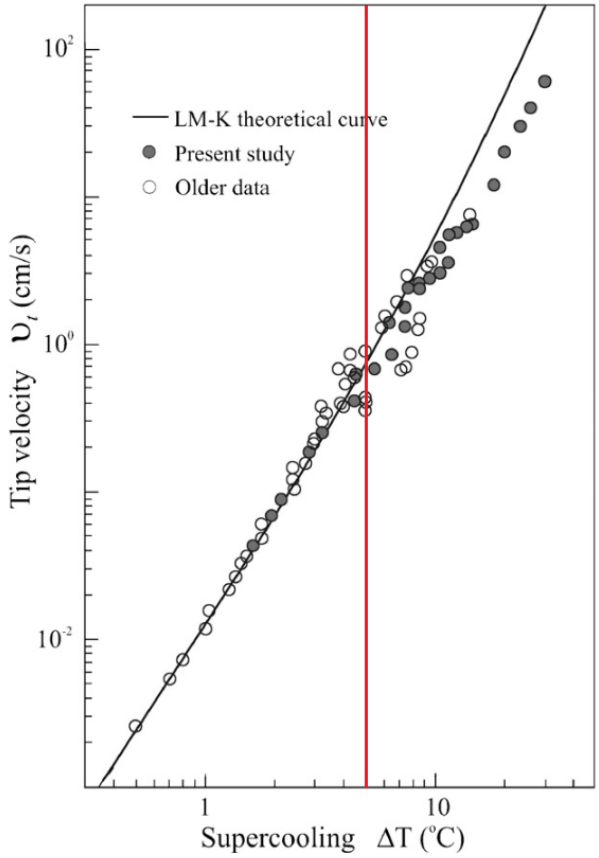


Figure 14: Comparison between experimental data and the LM-K theory (in solid line). Filled or unfilled correspond to different experimental data (the filled ones to Shibkov's study, and the unfilled ones to the previous analysis. Based on the figure from Shibkov et al. (2003). It is shown how below a certain supercooling temperature $\Delta T$ = 5 K, drawn as a red line, the LM-K theory is valid and beyond there is a discrepancy with the experimental data.

*The Langer and Müller-Krumbhaar (LM-K) theory*

The LM-K theory finds a solution, in steady state, for a crystal in the form of a paraboloid of revolution, in a dendrite shape form, that grows with a constant velocity of its tip, $v_t$. This solution is represented overlaying experimental data in Fig. 14.

The LM-K theory establishes a stability constant $\sigma = 1/(4\pi^2) = 0.0253$ which determines the tip radius $r_t$ and growth rate $v_t$ for a given supercooling $\Delta T_{sc}$ independent of the time of the dendrite evolution.

As described in Shibkov et al. (2004), in Ivantsov's solution the dimensionless supercooling temperature is defined as follows:

$$\Delta = \frac{\Delta T_{sc} \cdot c_{p,w}}{h_{fus}} \tag{12}$$

where $c_{p,w}$ is the heat capacity of water and $h_{fus}$ is the enthalpy of fusion. This dimensionless supercooling temperature, $\Delta$ is related to Péclet adimensional number with the following expression:

$$\Delta = p_e \cdot \exp(p_e) \cdot \int_{p_e}^{\infty} \exp(-x)/x \, dx \tag{13}$$

The *Péclet* number is defined as the ratio of the rate of advection (convection) to the rate of diffusion, and it is given by the formula:

$$p_e = (v_t \cdot r_t)/(2 \cdot \alpha_w) \tag{14}$$

where $\alpha_w$ is the thermal diffusivity.

The stability constant of the LM-K theory is equal to:

$$\sigma = 2 \cdot \alpha_w \cdot d_0/(v_t \cdot r_t^2) \tag{15}$$

where $d_0$ is the capillary length (which determines the surface tension forces' radius of action, calculated with the $T_m$ is the melting temperature, as follows:

$$d_0 = T_m \cdot \gamma_{iw} \cdot c_{p,w}/h_{fus}^2 \tag{16}$$

## 3.7 Population Balance Equations

### 3.7.1 Introduction

To investigate the size distribution of ice particles inside the crystallizer it is necessary to introduce the concept of Population Based Equationss (PBEs).

The PBEs, also referred to in the literature as Population Based Models (PBMs) are a set of integro-differential equations which describe the evolution of a specific characteristic of a population of particles, in our case, the size or volume. Our assumption is that crystals can be characterised by a single length parameter, denoted as $L$. This assumption implies the presence of a one-dimensional particle size distribution, represented as $f(L)$. Since $f$ is a density function, $f(L)dL$ represents the number of ice particles -by unit volume- of size between $L$ and $L + dL$ (Mazzotti et al., 2018).

This mathematical formulation is necessary to be implemented in our CFD environment because, regardless of the CFD mesh size chosen, the size of ice particles will always be smaller and therefore cannot be directly modelled. Thus, a mathematical approach using the PBEs must the used to assess the evolution of ice particles' size and distribution.

The proper consideration of ice particles' size and distribution inside the crystallizer is important for a thorough evaluation. Not only is it essential for accurately evaluating the rheological properties of the ice slurry, but also for calculating the particle fluid interaction forces, such as the drag force. These considerations directly influence the evolution of the crystallization process inside the crystallizer.

The calculation of the ice crystal size includes different phenomena like nucleation, growth, aggregation and breakage as represented visually in Fig. 15. The PBE formulation considered reads:

$$\frac{\partial f(L,t)}{\partial t} + \nabla[\overrightarrow{v_s} f(L,t)] + \frac{\partial[G(L)f(L,t)]}{\partial L} = Agg(L,t) + Bre(L,t) + Nuc(L,t) \tag{17}$$

The terms of the PBE have the following significance related to the ice crystal evolution processes:

- The first term of the left side of the equation $\frac{\partial f(L,t)}{\partial t}$ represents the rate of change of the number density of particles with respect to time.
- The second term of the left side of the equation $\nabla[\overrightarrow{v_s} f(L,t)]$, represents the advection of particles in the spatial (external) coordinate dimension. It describes how the number density of particles changes as a function of the external coordinates.
- The third term of the left-side of the equation $\frac{\partial[G(L)f(L,t)]}{\partial L}$, represents the growth rate term for particles.
- The first term of the right side of the equation, $Agg(L,t)$, represents the aggregation term of particles, also called coalescence. It accounts for the formation of larger particles through the collision and sticking together of smaller particles.
- The second term of the right side of the equation $Bre(L,t)$, represents breakage or *attrition* term of particles. It accounts for the fragmentation of larger particles into smaller ones due to external forces or collisions with other particles or with domain limits.
- The third term of the right side of the equation $Nuc(L,t)$, considers the rate at which the particles of size $L$ are nucleated.

These terms together describe the evolution of the particle size distribution over time and capture the various processes that can occur in a population of ice particles.

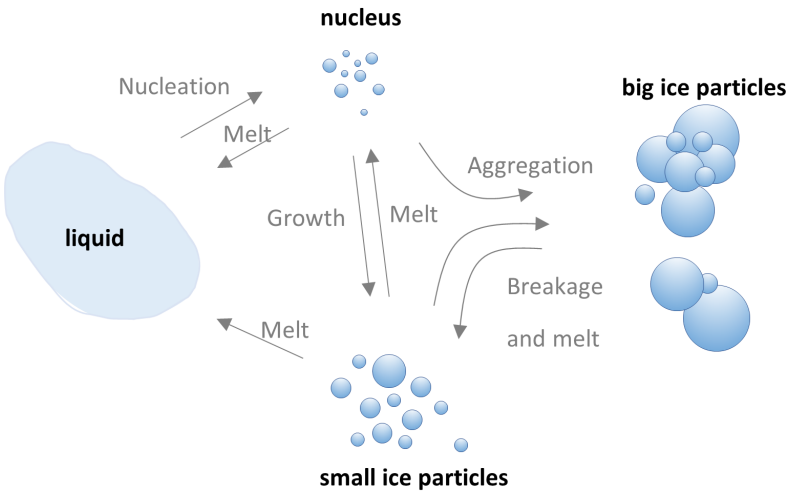


Figure 15: Dynamics of ice crystal based on Du et al. (2023)

### 3.7.2 PBE Growth rate term

Although specific equations for crystal growth rate for PBE have been found in the literature review (Du et al., 2023, Xu et al., 2014, 2018), the preference is to articulate the growth rate equation by deriving it from the growing rate function outlined in section 3.6.3 into a growth rate function.

### 3.7.3 PBE Aggregation term

The aggregation equation reaction is defined as:

$$Agg(L,t) = \frac{1}{2}\int_0^L \alpha(L-L',L')\cdot f(L-L',t)\cdot(L,t)\,dL' - \int_0^\infty \alpha(L,L')\cdot f(L,t)\cdot f(L',t)\,dL' \tag{18}$$

The first part of Eq. accounts for the aggregation of ice particles of $L-L'$ and $L'$ sizes, resulting in particles of size $L$. The second term accounts for the loss of particles of size $L$ by the aggregation of other particles of other sizes. The coefficient $\alpha(L-L',L')$ is the aggregation rate between particles of sizes $L-L'$ and $L'$, merging into a particle size $L$.

Aggregation is a physical process that can be sequenced in two steps: the collision of two particles, and the sticking or fusion of these (Xu et al., 2014). Therefore, the aggregation coefficient $\alpha$ is the product of both coefficients: the collision frequency $a$, and a sticking coefficient $a'$.

The collision of two particles in a fluid is a process which depends on the particle to particle forces and particle-fluid interaction.

When the long-range forces between the particles can be discarded, and the particles are small enough to avoid influencing the fluid phase or being disturbed by fluid shear, then the collision frequency can be characterised by the Brownian motion, which is commonly described as the random fluctuations or movements of particles suspended in a medium as described in the following Eq. 19:

$$a_b(L,L') = \frac{2K_BT}{3\nu}\cdot\frac{(L+L')^2}{LL'} \tag{19}$$

where $K_B$ is the Boltzamnn's constant 1 380649e$^{-23}$ in J/K, $T$ the absolute temperature of the fluid in which the particles are colliding in K; and $\nu$ is the fluid kinematic viscosity in J s/kg.

When particles larger enough to be influenced by the fluid flow, the Brownian motion assumption is not valid anymore, and the aggregation coefficient should be calculated with the following expression, which considers the turbulent dissipation rate $\epsilon$ in W/kg:

$$a_\epsilon(L,t) = \frac{4}{3}\cdot\left(\frac{3\pi}{10}\right)^{1/2}\cdot\left(\frac{\epsilon}{\nu}\right)^{1/2}\cdot(L+L')^3 \tag{20}$$

For the crystallizer the Eq. 20 based on the turbulence dissipation rate would be optimal.

The sticking coefficient $a'$ will analysed in future work.

### 3.7.4 PBE Breakage term

The breakage equation reaction is defined as:

$$Bre(L,t) = \int_L^\infty v(L')\cdot b(L')\cdot p(L|L')\cdot f(L',t)\,dL' - b(L)\cdot f(L,t) \tag{21}$$

The first part of Eq. 21 accounts for the formation of new ice particles of size $L$, broken from a larger particle of size $L'$ , resulting in particles of size $L$. The second term accounts for the loss of particles of size $L$ by the breakage into other smaller particles. The coefficient $b(L')$ accounts for the breakage rate between particles of size $L'$ into two particles of size $L$ and its difference $L'-L$.

$$b(L') = C_1\frac{\epsilon^{1/3}}{(1+\Gamma_{ice})\cdot\left(\frac{6L}{\pi}\right)^{2/9}}exp\left[-C_2\frac{\gamma_{iw}\cdot(1+\alpha)^2}{\rho_i\epsilon^{2/3}\cdot\left(\frac{6L}{\pi}\right)^{5/9}}\right] \tag{22}$$

where $\gamma_{iw}$ is the surface tension, mN/m; $\Gamma_{ice}$ is the mass ice fraction,%; $\rho_i$ is the density of ice slurry, kg/m$^3$; and $C_1$ and $C_2$ are breakage constants with values 0.00481 and 0.08 respectively.

The distribution function denoted as $p(L|L')$, defines the probability of a fragment with size $L$ of being generated from the breakage of an $L'$ sized particle. This probability is influenced by various factors, including particle properties such as strength or morphology.

### 3.7.5 PBE Nucleation term

The nucleation equation will be defined by deriving the nucleation equation of section 3.6.2 into a frequency of nucleation.

## 3.8 Coupling CFD and PBE

The first exploratory efforts to develop CDF models for various crystallizers developed in SPF, uniquely focusing on the fluid dynamic aspects, have commenced. The main goal was to analyse turbulence and fluid flow patterns, the streamlines, within different crystallizer designs. The different crystallizer designs preliminary analysed are flow-based crystallizers with different *turbulence enhancer*s:

- Crystallizer with no turbulence enhancer.
- Crystallizer with water-jet turbulence enhancer.
- Crystallizer with double jacket water-jet turbulence enhancer.

This analysis aimed to provide an initial understanding of turbulence, a critical factor in processes involving heat and mass transfer, as in the ice slurry formation. Turbulence can be measured by means of the *turbulent kinetic energy* magnitude, TKE, in $m^2/s^2$ or equivalently in J/kg.

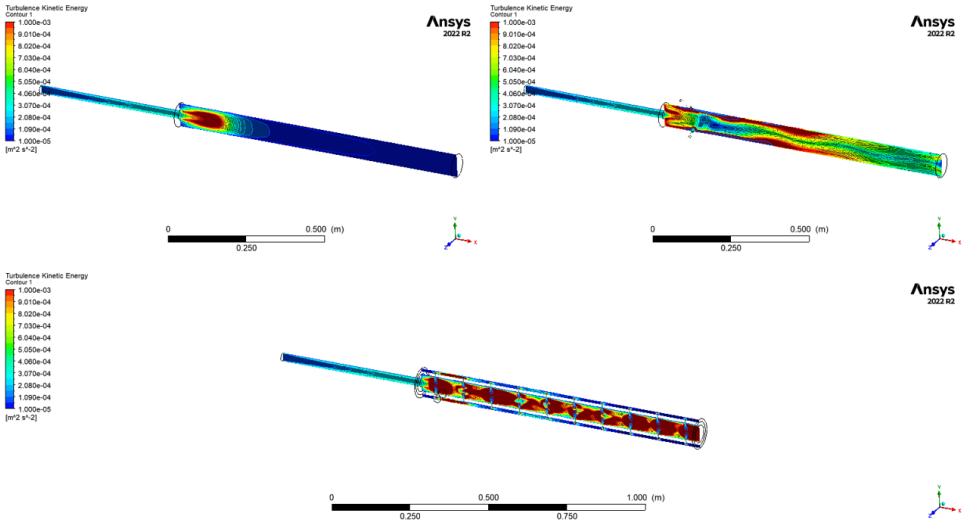


Figure 16: General view of TKE for three different crystallizers designs. Left up: (A) Crystallizer with no turbulence enhancer. Right up: (B) Crystallizer with water-jet turbulence enhancer. Down: (C) Crystallizer with double jacket water-jet turbulence enhancer.

In Fig. 16, Fig. 17, the TKE of three different crystallizers has been plotted. Fig. 17 is a zoom of Fig. 16. In these figures, it is shown that the crystallizer with no turbulence enhancer (left up in figures) exhibits low TKE values beyond a specific point along the crystallizer length (the turbulence generated at the inlet expansion dissipates from 15% of the crystalliser length onward). In the crystallizer with water-jet turbulence enhancer (right up in figures), TKE is better distributed but concentrated on walls. The concentration of TKE along the walls can be attributed to the angle at which water jets enter the crystallizer. Specifically, the water jets are introduced at an angle that induces swirls along the crystallizer, particularly in close proximity to the walls. This angular entry of water creates a swirling motion, leading to increased turbulence and higher concentrations of TKE along the crystallizer walls. The crystallizer with double jacket water-jet turbulence enhancer, (down in figures), has a better distribution along and across the crystallizer which is beneficial for homogenizing the biphasic flow and enhancing crystal growth.

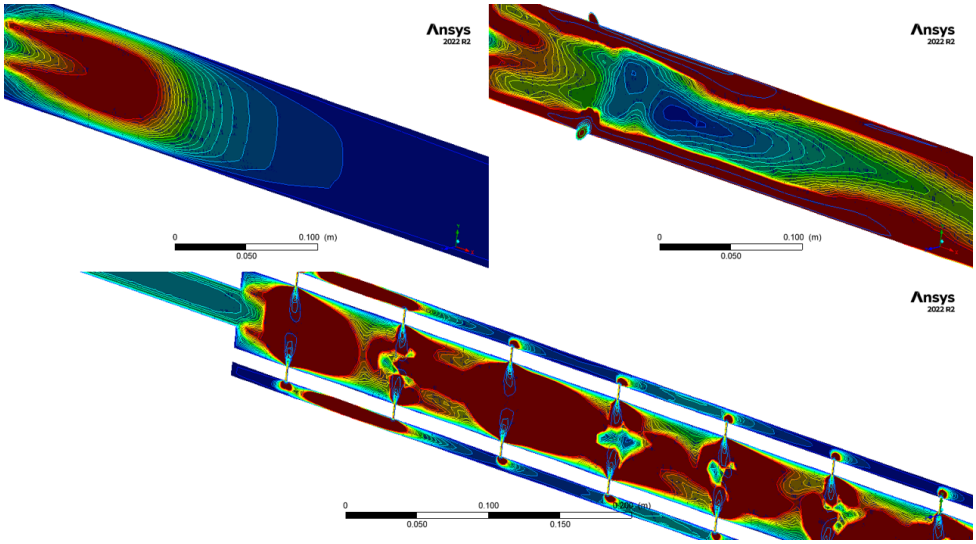


Figure 17: The detailed view of TKE for three different crystallizer designs reveals notable differences. It is evident from CFD results that both designs (B) and (C) exhibit enhanced turbulence, with the turbulence being more evenly distributed in design (C).

While these models are currently in a preliminary stage, they have already offered initial qualitative insights, aligning with qualitative experimental observations and facilitating progress in technology development.

## 3.9 Experimental conceptualization

For validation of the different numerical models: fluid flow CFD model or coupled crystal growth and fluid flow CFD model, several non-intrusive Quantitative Flow Visualization (QFV) techniques are foreseen.

### Particle Image Velocimetry (PIV)

For validation of the fluid flow CFD model (without crystallization) PIV technique is foreseen. PIV would provide accurate information of, at least, flow patterns, but in its complete quantitative technique, also fluid flow velocity fields and turbulence statistics.

PIV consists on a light sheet formed by means of a laser light which illuminates particles inside the fluid flow, twice with a short time interval, in order to obtain from those, flow velocities and patterns. For velocity calculation, the particle image of each camera is subdivided into small areas, called interrogation windows, where the average particle displacement is determined. From the known time difference and the measured displacement in each direction, the velocity components are calculated. From one velocity field, a range of spatial derivatives can be calculated, such as vorticity and shear stress. Ensemble statistics provide additional information like turbulent kinetic energy or Reynolds stresses. These measurements and postprocessing will be carried out using LaVision specialised software.

For validation of the coupled crystal growth and fluid flow CFD model other non-intrusive QFV techniques are foreseen. PIV is not an option here due to the possibility that the scattering efficiency of ice crystals could become too high and could saturate and damage the PIV camera sensor. One QFV alternative technique foreseen is called BSI.

### Backlight Shadow Imaging (BSI)

BSI is very suitable for visualizing and tracking particles, droplets and other structures as crystal ice structures. The technique is based on a pulsed backlight illumination and a high-magnification camera, which captures the size, shape, orientation, and perimeter of individual particles in the Region of Interest (RoI), in a defined

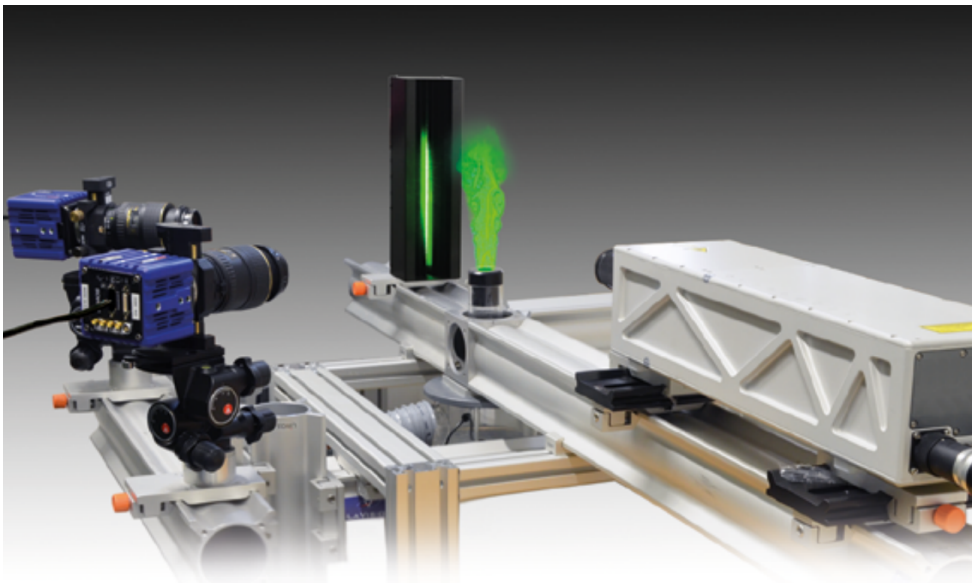

Figure 18: Particle Image Velocimetry (PIV) setup. From LaVision

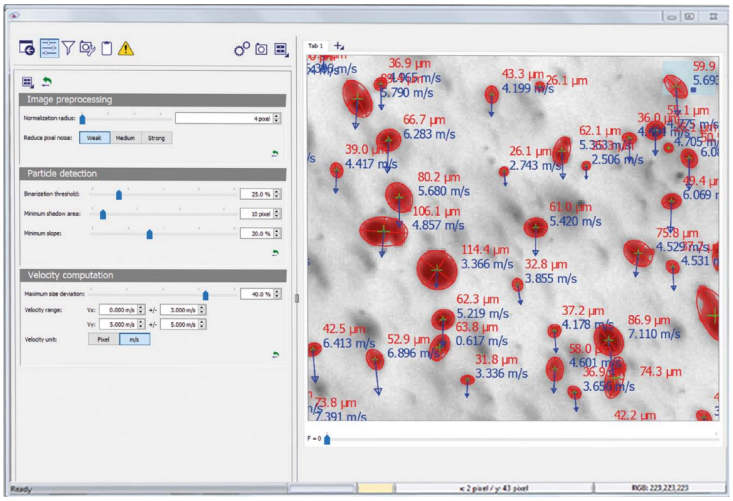


Figure 19: Backlight Shadow Imaging (BSI). From LaVision

focal plane and depth of field. The BSI technique is independent of the shape and material of the particles, even transparent, such as ice crystals, that can be detected inside its probe volume (the inside Depth of Field (DoF)). The light source can be a pulsed laser with special illumination optics or a flash lamp, depending on the velocity of the particles. When it is foreseen, as it is in our investigation, the analysis of size-dependent particle velocities, a double pulse laser or flash lamp, combined with a double frame camera, is normally used. Depending on the RoI a different camera and high-magnification lens is required. With this technique, it will be possible to obtain measured quantities of size, shape and velocities of individual particles and their distribution, complementary to those obtained through CFD, allowing to validate the model.

# 4 National/International cooperation

In the current stage of the project *ModIceCrys*, the national/international cooperation level has been initiated:

- A collaboration with Assis. Prof. Dr. Thomas Schutzius, through an SNF project *FRIO: Fundamentals of Recalescent Freezing on Immersed Nano-engineered Surfaces: The Influence of External Flow and Ultrasonic Fields* was in place last year. This proposal was submitted and approved when Dr. Thomas Schutzius was in Institut für Energietechnik - ETH Zürich. Currently, Prof. Dr. Thomas Schutzius is at Berkeley University in California (United States) from where he leads as Principal Investigator (PI) the FRIO project. Dr. Daniel Carbonell is the Co-Investigator (CoI) ensuring thus a proper know-how transfer.

- Firsts discussions with Prof. Dr. Filippo Coletti from the Department of Mechanical and Process Engineering at ETH Zürich were conducted for the establishment of a collaboration agreement for experimental methods on fluid mechanics of solid particles within turbulent flows.

- SPF is a partner in an inter-continental project funded by the Department of Energy (DOE) from United States where the ice slurry using the supercooling method is applied to thermo-electrical energy storage solutions using a Carnot battery concept. The ice crytallizer develop for that project will be used in ModIceCrys as first design for testing the CFD models.

# 5 Publications and conference contributions

So far, neither publications nor conference contributions have been generated.

# 6 Evaluation of 2023 and outlook of 2024

The project *ModIceCrys* started in November 2022. During 2023, a comprehensive review of supercooling method and crystallization has been conducted. This comprehensive review has given valuable insights into nucleation and crystal growth models that will be employed in both the Population Balance Models (PBM) and the coupled multiscale Computational Fluid Dynamics (CFD) for the crystallizer model.

The analysis of the PBM equations to be implemented and its integration into the CFD model have progressed. The literature review on this topic has been almost completed, but its full implementation into a standalone model is pending.

Simultaneously, efforts have commenced to develop CFD models, specifically focusing on the fluid dynamic aspects, for various crystallizers' prototypes developed in previous SPF's projects. The primary objective is to isolate and understand the unique characteristics of fluid dynamic flows, specifically the turbulence distribution, in each crystallizer's prototype. While these models are currently in a preliminary stage, they have already offered initial qualitative insights, aligning with experimental observations and facilitating progress in technology development.

Looking ahead to the year 2024, the plan is to conclude the integration of crystallization models within the PBMs, and develop the PBM standalone model for ice growth, which is planned to be done in the next

few months. Once finished, it is planned to develop deeper the fluid dynamic model of the crystallizer, with foresight on the development of the experimental setup. The two CFD software: ANSYS Fluent or OpenFOAM, are still under consideration for this purpose depending on the progress and advancements in ice slurry modelling that have been made so far in both CFD environments. Concurrently, the experimental phase for the fluid dynamic component is foreseen to begin next year. This experimental data will play a crucial role in validating the aforementioned fluid dynamic models, creating a symbiotic relationship between theoretical and experimental aspects of the research.

# References


Akhtar, S., Xu, M., and Sasmito, A. P. (2021). A Novel Crystal Growth Model with Nonlinear Interface Kinetics and Curvature Effects: Sensitivity Analysis and Optimization. *Crystal Growth & Design*, 21(6):3251–3265.

Beaupere, N., Soupremanien, U., and Zalewski, L. (2018). Nucleation triggering methods in supercooled phase change materials (PCM), a review. *Thermochimica Acta*, 670:184–201.

Burton, W. K., Cabrera, N., Frank, F. C., and Mott, N. F. (1951). The growth of crystals and the equilibrium structure of their surfaces. *Philosophical Transactions of the Royal Society of London. Series A, Mathematical and Physical Sciences*, 243(866):299–358. Publisher: Royal Society.

Cahn, J. W., Hillig, W., and Sears, G. (1964). The molecular mechanism of solidification. *Acta Metallurgica*, 12(12):1421–1439.

Carbonell, D., Shubert, M., Frandsen, J. R., Erb, K., Laib, L., and Munari, M. (2022). Development of supercoolers for ice slurry generators using icephobic coatings. *Internationa Journal of Refrigeration*, 144:90 – 98.

Carbonell, D., Theiler, D., and Tamm, A.-K. (2023). Slurry-Store - Experimental and numerical investigations of ice slurry storages. Technical report, SPF-OST.

Dorsey, N. E. (1948). The Freezing of Supercooled Water. *Transactions of the American Philosophical Society*, 38(3):247–328. Publisher: American Philosophical Society.

Du, Q., Chen, M., Song, W., Qin, K., and Feng, Z. (2023). Investigation on the evolution of ice particles and ice slurry flow characteristics during subcooling release. *International Journal of Heat and Mass Transfer*, 209:124008.

Fernandez, R. and Barduhn, A. (1967). The growth rate of ice crystals. *Desalination*, 3(3):330–342.

Fisher, J. C., Hollomon, J. H., and Turnbull, D. (1949). Rate of Nucleation of Solid Particles in a Subcooled Liquid. *Science*, 109(2825):168–169. Publisher: American Association for the Advancement of Science.

Gibbs, J. W. (1879). On the Equilibrium of Heterogeneous Substances. Publisher: Heidelberg University Library.

Giberti, F. (2014). *Computer Simulations of Homogeneous Nucleation*. Doctoral Thesis, ETH Zurich. Accepted: 2017-06-14T01:22:52Z.

Ivantsov, G. P. (1947). Temperature field around a spherical, cylindrical, and needle-shaped crystal, growing in a pre-cooled melt. Technical report. Publication Title: Temperature field around a spherical Volume: 58 ADS Bibcode: 1985tfas.rept..567I.

Kallungal, J. P. and Barduhn, A. J. (1977). Growth rate of an ice crystal in subcooled pure water. *AIChE Journal*, 23(3):294–303.

Kauffeld, M., Kawaji, M., and Egolf, P. W. (2005a). *Handbook on Ice Slurries - Fundamentals and Engineering*. International Institute of Refrigeration (IIR), $1^{st}$ edition.

Kauffeld, M., Kawaji, M., and Egolf, P. W. (2005b). *Handbook on ice slurries: fundamentals and engineering*. International Institute of Refrigeration, Paris. OCLC: 833158681.

Kauffeld, M., Wang, M. J., Goldstein, V., and Kasza, K. E. (2010). Ice slurry applications. *International Journal of Refrigeration*, 33(8):1491–1505.

Kozawa, Y., Aizawa, N., and Tanino, M. (2005). Study on ice storing characteristics in dynamic-type ice storage system by using supercooled water.: Effects of the supplying conditions of ice-slurry at deployment to district heating and cooling system. *International journal of refrigeration*, 28(1):73–82.

Kurz, W. (2017). *50 Year's Solidification Research The Dendrite Growth Problem between Brighton and Old Windsor*.

Langer, J. and Müller-Krumbhaar, J. (1977). Stability effects in dendritic crystal growth. *Journal of Crystal Growth*, 42:11–14.

Langer, J. S. and Müller-Krumbhaar, H. (1978). Theory of dendritic growth—I. Elements of a stability analysis. *Acta Metallurgica*, 26(11):1681–1687.

Langer, J. S., Sekerka, R. F., and Fujioka, T. (1978). Evidence for a universal law of dendritic growth rates. *Journal of Crystal Growth*, 44(4):414–418.

Libbrecht, K. G. (2017). Physical Dynamics of Ice Crystal Growth. *Annual Review of Materials Research*, 47(1):271–295. _eprint: https://doi.org/10.1146/annurev-matsci-070616-124135.

Mazzotti, M., Vetter, T., and Ochsenbein, D. R. (2018). Crystallization Process Modeling. In Hilfiker, R. and Raumer, M. V., editors, *Polymorphism in the Pharmaceutical Industry*, pages 285–304. Wiley, 1 edition.

Mouneer, T. A., El-Morsi, M. S., Nosier, M. A., and Mahmoud, N. A. (2010). Heat transfer performance of a newly developed ice slurry generator: A comparative study. *Ain Shams Engineering Journal*, 1(2):147–157.

Němec, T. (2013). Estimation of ice–water interfacial energy based on pressure-dependent formulation of classical nucleation theory. *Chemical Physics Letters*, 583:64–68.

Salvati Manni, L., Assenza, S., Duss, M., Vallooran, J. J., Juranyi, F., Jurt, S., Zerbe, O., Landau, E. M., and Mezzenga, R. (2019). Soft biomimetic nanoconfinement promotes amorphous water over ice. *Nature Nanotechnology*, 14(6):609–615. Number: 6 Publisher: Nature Publishing Group.

Shibkov, A., Golovin, Y., Zheltov, M., Korolev, A., and Leonov, A. (2003). Morphology diagram of nonequilibrium patterns of ice crystals growing in supercooled water. *Physica A: Statistical Mechanics and its Applications*, 319:65–79.

Shibkov, A., Zheltov, M., Korolev, A., Kazakov, A., and Leonov, A. (2005). Crossover from diffusion-limited to kinetics-limited growth of ice crystals. *Journal of Crystal Growth*, 285(1-2):215–227.

Shibkov, A. A., Zheltov, M. A., Korolev, A. A., Kazakov, A. A., and Leonov, A. A. (2004). Effect of surface kinetics on the dendritic growth of ice in supercooled water. *Crystallography Reports*, 49(6):1056–1063.

Stamatiou, E., Meewisse, J. W., and Kawaji, M. (2005). Ice slurry generation involving moving parts. *International Journal of Refrigeration*, 28(1):60–72.

Wang, T., Lü, Y., Ai, L., Zhou, Y., and Chen, M. (2019). Dendritic Growth Model Involving Interface Kinetics for Supercooled Water. *Langmuir*, 35(15):5162–5167. Publisher: American Chemical Society.

Xu, A., Liu, Z., Zhao, T., and Wang, X. (2014). Population balance model of ice crystals size distribution during ice slurry storage. *International Journal of Air-Conditioning and Refrigeration*, 22(02):1440001. Publisher: World Scientific Publishing Co.

Xu, D., Liu, Z., Cai, L., Tang, Y., Yu, Y., and Xu, A. (2018). A CFD-PBM approach for modeling ice slurry flow in horizontal pipes. *Chemical Engineering Science*, 176:546–559.

Zhang, P. and Ma, Z. W. (2012). An overview of fundamental studies and applications of phase change material slurries to secondary loop refrigeration and air conditioning systems. *Renewable and Sustainable Energy Reviews*, 16(7):5021–5058.